





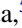

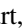


Frustration on a centered pyrochlore lattice in metal-organic frameworks

Rajah P. Nutakki, Richard Röß-Ohlenroth, Dirk Volkmer, Anton Jesche, Hans-Albrecht Krug von Nidda, Alexander A. Tsirlin, Philipp Gegenwart, Lode Pollet, Ludovic D. C. Jaubert

Angaben zur Veröffentlichung / Publication details:

Nutakki, Rajah P., Richard Röß-Ohlenroth, Dirk Volkmer, Anton Jesche, Hans-Albrecht Krug von Nidda, Alexander A. Tsirlin, Philipp Gegenwart, Lode Pollet, and Ludovic D. C. Jaubert. 2023. "Frustration on a centered pyrochlore lattice in metal-organic frameworks." *Physical Review Research* 5 (2): L022018. <https://doi.org/10.1103/physrevresearch.5.L022018>.

Frustration on a centered pyrochlore lattice in metal-organic frameworks

Rajah P. Nutakki ^{1,2}, Richard Röß-Ohlenroth ³, Dirk Volkmer ³, Anton Jesche ⁴, Hans-Albrecht Krug von Nidda ⁵, Alexander A. Tsirlin ⁴, Philipp Gegenwart ⁴, Lode Pollet ^{1,2} and Ludovic D. C. Jaubert ⁶

¹Arnold Sommerfeld Center for Theoretical Physics, University of Munich, Theresienstrasse 37, D-80333 München, Germany

²Munich Center for Quantum Science and Technology (MCQST), Schellingstrasse 4, D-80799 München, Germany

³Chair of Solid State and Materials Chemistry, Institute of Physics, University of Augsburg, D-86159 Augsburg, Germany

⁴Experimental Physics VI, Center for Electronic Correlations and Magnetism, Institute of Physics, University of Augsburg, D-86159 Augsburg, Germany

⁵Experimental Physics V, Center for Electronic Correlations and Magnetism, Institute of Physics, University of Augsburg, D-86159 Augsburg, Germany

⁶CNRS, Université de Bordeaux, LOMA, UMR 5798, F-33400 Talence, France



(Received 5 November 2022; revised 2 February 2023; accepted 21 March 2023; published 1 May 2023)

Geometric frustration inhibits magnetic systems from ordering, opening a window to unconventional phases of matter. The paradigmatic frustrated lattice in three dimensions to host a spin liquid is the pyrochlore, although there remain few experimental compounds thought to realize such a state. Here, we go beyond the pyrochlore via molecular design in the metal-azolate framework $[\text{Mn}(\text{II})(\text{ta})_2]$, which realizes a closely related centered pyrochlore lattice of Mn spins with $S = 5/2$. Despite a Curie-Weiss temperature of -21 K indicating the energy scale of magnetic interactions, $[\text{Mn}(\text{II})(\text{ta})_2]$ orders at only 430 mK, putting it firmly in the category of highly frustrated magnets. Comparing magnetization and specific-heat measurements to numerical results for a minimal Heisenberg model, we predict that this material displays distinct features of a classical spin liquid with a structure factor reflecting Coulomb physics in the presence of charges.

DOI: [10.1103/PhysRevResearch.5.L022018](https://doi.org/10.1103/PhysRevResearch.5.L022018)

Over the last few decades, the theoretical study of magnetism on geometrically frustrated lattices has proven highly successful in identifying exotic states of matter, ranging from classical spin ice [1,2] to quantum spin liquids [3–5]. In three dimensions, the most well-studied frustrated lattice is arguably the pyrochlore lattice of corner-sharing tetrahedra. For the classical nearest-neighbor Ising and Heisenberg models on the pyrochlore lattice, the spin-liquid ground states have an elegant description in terms of an emergent $U(1)$ gauge field which leads to their characterization as Coulomb spin liquids [6,7], with excitations interacting via an effective Coulomb potential and characteristic pinch point singularities in the spin structure factor. The clearest experimental realization is found in the spin ice compounds $\text{Dy}_2\text{Ti}_2\text{O}_7$ and $\text{Ho}_2\text{Ti}_2\text{O}_7$ [8], where the local orientations of the spins and dipolar interactions introduce additional energetic (rather than purely entropic) Coulomb interactions, which in turn leads to a description of excitations in terms of magnetic monopoles [9]. In the Heisenberg case, recent experiments on the transition metal pyrochlore fluoride, $\text{NaCaNi}_2\text{F}_7$, find that it is well described by an $S = 1$ pyrochlore Heisenberg antiferromagnet (PHAF) and thought to realize a Coulomb-like phase [10]. Unfortunately, it is a recurrent theme for Heisenberg materials that further neighbor interactions, anisotropic exchanges, or

disorder perturbs the spin-liquid physics at low temperatures [2,11–14].

Recently, metal-organic frameworks have emerged as a class of materials for realizing strongly magnetically frustrated systems [15], offering a new avenue to realizing both familiar and novel geometrically frustrated lattices in the laboratory. Here, our focus is on the metal-azolate frameworks $[\text{M}(\text{II})(\text{ta})_2]$, where $\text{M}(\text{II})$ is a divalent metal ion and $H\text{-ta} = 1H\text{-}1, 2, 3\text{-triazole}$, which exhibit a diamond net with vertices made of M -centered (MM_4) tetrahedra (Fig. 1), offering the exciting possibility to engineer novel magnetic structures by inserting additional, magnetically active ions into the pyrochlore lattice. However, so far only a handful of works have addressed their magnetic properties [16–21].

In this Letter, we explore the potential of metal-azolate frameworks in the context of frustrated magnetism by studying $[\text{Mn}(\text{ta})_2]$, which realizes a centered pyrochlore lattice. Using a combination of specific-heat and magnetic measurements, *ab initio* calculations, Monte Carlo (MC) simulations, exact diagonalization, and analytical insights, we predict the existence of a finite temperature regime around $T \approx 2$ K where we expect to find the hallmarks of an underlying classical spin liquid in the *minimal* model. The correlations in this spin liquid can be understood in the Coulomb framework as a dense fluid of charges created by the center spins, reminiscent of the monopole fluid studied in the context of spin ice [22,23].

Minimal model. Adapting the synthesis procedure of Ref. [24], $[\text{Mn}(\text{ta})_2]$ was prepared as a white powder sample. Rietveld refinements of x-ray diffraction data find that

Published by the American Physical Society under the terms of the Creative Commons Attribution 4.0 International license. Further distribution of this work must maintain attribution to the author(s) and the published article's title, journal citation, and DOI.

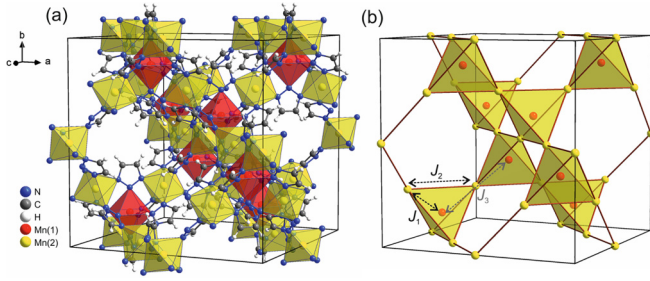


FIG. 1. (a) Combined ball-and-stick and polyhedra model of cubic $[\text{Mn(II)(ta)}_2]$ highlighting the positions of divalent octahedrally coordinated Mn ions arranged in a diamond-type lattice (CSD code: HEJQEV). The metal centers differ with respect to their special crystallographic positions and coordination environments: Mn(1) is located on Wyckoff position $8b$ (site symmetry $\bar{4}3m$), coordinated exclusively by the N2 donor atoms of the μ_3 -bridging triazolate linker; Mn(2) is found at Wyckoff position $16d$ (site symmetry $\bar{3}m$), coordinated exclusively by N1 or N3 donor atoms. (b) Schematic representation of the centered pyrochlore lattice with magnetic exchange paths for first [J_1 , Mn(1)-Mn(2), 3.929 Å], second [J_2 , Mn(2)-Mn(2), 6.416 Å], and third [J_3 , Mn(1)-Mn(1), 7.858 Å] neighbors. Mn(1) and Mn(2) are respectively labeled center (orange) and corner (yellow) spins.

$[\text{Mn(ta)}_2]$ has the cubic symmetry of the $Fd\bar{3}m$ space group [17] which we confirm through high-resolution x-ray powder diffraction at 5 K. Since the $3d$ valence band of high-spin Mn(II) ions is half filled, we expect its magnetic moment to be isotropic. Previous conductivity measurements together with periodic density functional theory (DFT) band-structure calculations [25] classified this compound as a wide-band-gap semiconductor with a band gap $\Delta = 3.1$ eV $\equiv 36\,000$ K. We therefore consider $[\text{Mn(ta)}_2]$ an insulator at temperatures $T \ll \Delta$. To assess the relevance of different exchange pathways (Fig. 1), we performed DFT calculations assuming isotropic exchanges for high-spin $3d^5$ Mn(II) ions between first (J_1), second (J_2), and third (J_3) neighbors [see Fig. 1(b) and Supplemental Material [26]]. We obtain that $J_1^{\text{DFT}} \sim 2\text{--}4$ K and $\gamma^{\text{DFT}} \equiv J_1^{\text{DFT}}/J_2^{\text{DFT}} \approx 1.3\text{--}1.65$. The fact that J_1^{DFT} and J_2^{DFT} are of the same order of magnitude is likely due to the similar exchange pathways, traversing either two or three nitrogen ions respectively along the triazolate ligand. On the other hand, no such pathway is available beyond second neighbors, hence $|J_3^{\text{DFT}}| < 0.01$ K $\ll J_1^{\text{DFT}}, J_2^{\text{DFT}}$. Owing to this separation of scales, it suffices to define a minimal model (CPy) on the centered pyrochlore lattice with only first and second neighbor isotropic couplings,

$$H = J_1 \sum_{\langle ij \rangle} \mathbf{S}_i \cdot \mathbf{S}_j + J_2 \sum_{\langle\langle ij \rangle\rangle} \mathbf{S}_i \cdot \mathbf{S}_j - \mu_0 \mathbf{H} \cdot \sum_i \mathbf{S}_i. \quad (1)$$

Confirming that $[\text{Mn(ta)}_2]$ is described by Hamiltonian (1) requires the appropriate theoretical tools. Fortunately, owing to the large magnetic moment $S = 5/2$ we can resort to classical Monte Carlo simulations, which have proven to be powerful techniques to describe magnetic properties of pyrochlore materials capable of capturing long-range order as well as unconventional correlations of spin liquids [2,27–31]. Continuous-spin models cannot, however, reproduce specific heat at very low temperatures because entropy is ill defined.

There, one needs to consider the discrete nature of quantum spins via, e.g., exact diagonalization (ED). Since ED for $S = 5/2$ is particularly costly in computer time and memory, we will restrict calculations to a single tetrahedral unit of five spins, fitted to high-temperature experimental data. Such an approximation shall provide an independent estimate of the energy scales, to be compared with parameters obtained from DFT and Monte Carlo simulations. In the rest of this Letter, \mathbf{S}_i will denote a three-component classical spin of length $|\mathbf{S}_i| = 5/2$, except when analyzing specific-heat data where \mathbf{S}_i is a quantum $S = 5/2$ spin.

Comparison between experiment and theory. To explore the magnetism of $[\text{Mn(ta)}_2]$, we measured magnetic susceptibility over three decades in temperature. Fitting the high-temperature regime ($T > 200$ K) of the susceptibility χ with a Curie-Weiss law [Fig. 2(a)], we obtain an effective magnetic moment $\mu_{\text{eff}} = 6.05\mu_B$ per Mn ion and a Curie-Weiss temperature $\Theta_{\text{CW}} = -21$ K. These values agree with a previous report [17] ($5.8\mu_B$ and -21.9 K, respectively) and with the expected size of the magnetic moment $g_S \sqrt{S(S+1)} = 5.9\mu_B$ which is a stable value for a Mn(II) ion with high-spin $3d^5$ electronic configuration. Θ_{CW} indicates sizable antiferromagnetic interactions. However, our specific-heat measurements do not find a transition until a low $T_c = 0.43$ K [Fig. 2(c)]. For comparison, the degree of frustration $f \equiv \frac{|\Theta_{\text{CW}}|}{T_c} = 49$ is of the same order as the one of the celebrated Kitaev materials [13,32] and substantially larger than the one of most rare-earth pyrochlore oxides [2,11,12]. It means that not only does $[\text{Mn(ta)}_2]$ offer an unexplored geometry, but one can also expect a sizable temperature range above T_c where frustration is important.

Our main result is the agreement between experiments and Monte Carlo simulations for the (i) magnetic susceptibility in Fig. 2(a), and (ii) magnetization curves in Fig. 2(b), using coupling parameters that confirm the DFT estimates, $J_1^{\text{MC}} = 2.0$ K and $\gamma^{\text{MC}} = 1.51 \pm 0.15$. Further support for this claim is seen in the fit of the specific heat [Fig. 2(c)]: The bump at ~ 4 K is also consistent with finite-temperature exact diagonalization for $J_1^{\text{ED}} = 1.95$ K and $\gamma^{\text{ED}} \sim 1.75$ [Fig. 2(c)]. While the value of γ^{ED} should only be considered as a qualitative estimate, the ED results indicate that the bump at 4 K corresponds to a growth of the correlation length beyond a single frustrated unit. The region $0.43 < T \lesssim 4$ K thus appears appropriate to support a potentially exotic magnetic structure, where frustrated correlations exist, but have not yet been destroyed by long-range order. We study the nature of this regime in the following.

The centered pyrochlore spin liquid. To show how the CPy model can host a spin liquid, it is convenient to rewrite Hamiltonian (1) as a sum over (centered) tetrahedra, with index α ,

$$H = \frac{J_2}{2} \sum_{\alpha} |\mathbf{L}_{\alpha}|^2 + \text{const}, \quad (2)$$

with

$$\mathbf{L}_{\alpha} = \gamma \mathbf{S}_{\alpha,c} + \sum_{m=1}^4 \mathbf{S}_{\alpha,m}, \quad (3)$$

where c labels the center spin while the sum over m runs over the four corner spins. The ground-state manifold is therefore defined by minimizing $L_{\alpha} = |\mathbf{L}_{\alpha}|$ on all units. For $\gamma \geq 4$, this

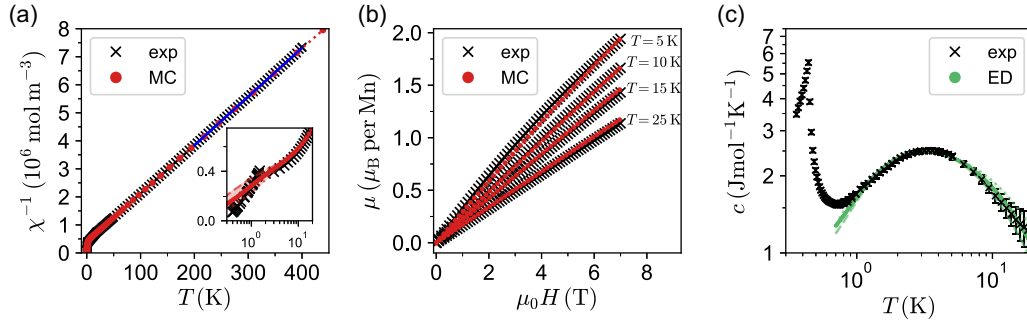


FIG. 2. Comparison between experiment and theory for $[\text{Mn}(\text{ta})_2]$. (a) Curie-Weiss fit (blue, for $T > 200$ K) of the inverse susceptibility χ^{-1} obtained from magnetization measurements $\chi = M/H$ (black) and MC simulations of over 41 000 spins (red). Inset: The inverse susceptibilities at low temperatures. The Curie-Weiss fit yields a Landé factor of $g = 2.05$. (b) Magnetization in an external field over a broad temperature range. MC simulations compare well to experimental magnetization measurements at $T > 1$ K for $J_1^{\text{MC}} = 2.0$ K, $\gamma^{\text{MC}} = 1.51 \pm 0.15$. (c) The specific heat of $[\text{Mn}(\text{ta})_2]$ displays a broad bump at ~ 4 K and a sharp peak at 0.43 K. The former is qualitatively reproduced by full diagonalization for $J_1^{\text{ED}} = 1.95$ K and $\gamma^{\text{ED}} \sim 1.75$ up to a rescaling by a factor of 0.8 along the y axis. In order to show the γ dependence of Hamiltonian (1), simulation curves in (a) and (c) are supplemented by dotted and dashed lines corresponding to $\pm 10\%$ variations of γ .

yields a long-range ordered ferrimagnet with $1/3$ saturated magnetization where $\mathbf{S}_{\alpha,i=1,\dots,4} = -\mathbf{S}_{\alpha,c}$. On the other hand, for $\gamma < 4$, the ground state is defined by the local constraint

$$\mathbf{L}_\alpha = 0, \quad \forall \alpha. \quad (4)$$

Such an energetic constraint, familiar from the kagome and pyrochlore lattices, is often used to define a classical spin liquid, provided order by disorder does not select an ordered state. A Maxwellian counting argument [33] gives the degrees of freedom D_n of these spin liquids. For the kagome, $D_3 = 0$ (which is famously marginally disordered), whereas $D_4 = N_u$ for the pyrochlore [33], where N_u is the number of units making up the lattice. In the CPy model, we find $D_5 = 3 N_u$ for $\gamma \sim 1$. Similarly, these spin liquids manifest themselves via a number of flat bands F_n as the ground state of their excitation spectrum [34]: $F_3 = 1$ out of 3 bands for kagome, $F_4 = 2$ out of 4 for pyrochlore, whereas $F_5 = 4$ flat bands out of 6 for $\gamma < 4$ in the CPy model (see Supplemental Material [26]). Therefore, the CPy model hints at a notably strong spin liquid, even more disordered than the extensively studied ones on kagome and pyrochlore. This is supported by our Monte Carlo simulations [35] showing that CPy lies in the middle of a disordered ground state (found for any $\gamma \lesssim 3$) which indicates that the ordering mechanism in $[\text{Mn}(\text{ta})_2]$ lies beyond our minimal CPy model. This is often the case in frustrated magnetism [2,11–13], where perturbations ultimately lift the ground-state degeneracy in materials. In this case, the largest perturbation is likely dipolar interactions with a nearest-neighbor strength of 270 mK. Adding these to the CPy model, we find ordering at 250 mK in MC simulations, where the ordered state is an unsaturated ferrimagnet with corner spins realizing a planar antiferromagnet on each tetrahedron with the remaining spin weight. Further details are provided in the Supplemental Material [26]. Our simulations show that the addition of dipolar interactions does not significantly modify the properties of the model in the regime $1 < T < 4$ K, where we expect the spin liquid to persist.

An emergent charge fluid. To better understand the nature of this spin liquid and its relation to known pyrochlore physics we look at the magnetic correlations, best visualized through

the structure factor in reciprocal space, $\mathcal{S}(\mathbf{q})$ [Figs. 3(a) and 3(b)]. We find that, in the regime $0 < \gamma < 2$, $\mathcal{S}(\mathbf{q})$ is characterized by finite width bowties, which are found to arise from the correlations between spins residing at the vertices of the tetrahedra. The magnetic structure evolves continuously in this regime, with the width of the bowties increasing with γ . This suggests that these correlations can be understood in the framework of the Coulomb phase on the pyrochlore lattice. Rewriting the constraint, Eq. (4), for each of the spin components $a \in \{x, y, z\}$ as

$$\sum_{m=1}^4 S_{\alpha,m}^a = -\gamma S_{\alpha,c}^a = \rho_\alpha^a, \quad (5)$$

we interpret ρ_α^a as a pseudoscalar (“magnetic”) charge, with a strength parametrized by γ . Hence, the Coulomb description is that of an effective field coupled to charges on the diamond lattice that break the zero-divergence constraint. For small γ , the charge concentration is low, so Debye-Hueckel theory [36,37] can be used to understand the spin correlations. In this regime, there will be entropic screening of the effective field, resulting in a Lorentzian form for its structure factor

$$\mathcal{B}_{aa}^a(q_a, q_b = 0, q_c = 0) \propto \frac{1}{q_a^2 + \kappa^2}, \quad (6)$$

where $a, b, c \in \{x, y, z\}$ and Debye-Hueckel theory predicts that $\kappa \propto \gamma$. At some value of γ , the charge concentration becomes large and we will need to account for additional corrections. Remarkably, we find that the prediction from Debye-Hueckel theory holds in MC simulations up to $\gamma \approx 1.25$ [see Fig. 3(c)]. Thus, the correct description for the regime relevant to $[\text{Mn}(\text{ta})_2]$, $\gamma^{\text{MC}} \approx 1.5$, is that of a moderately dense charge fluid, which is the Heisenberg model variant of a monopole fluid in spin ice. While this description accounts for the entropic selection of specific spin configurations, it does not account for energetic considerations necessary for a full effective description of the structure factor, such as which charge distributions enter the ground state.

Outlook. The CPy model, established as a minimal model for $[\text{Mn}(\text{ta})_2]$, displays a number of attractive features such as large, isotropic Heisenberg interactions, an unusually large

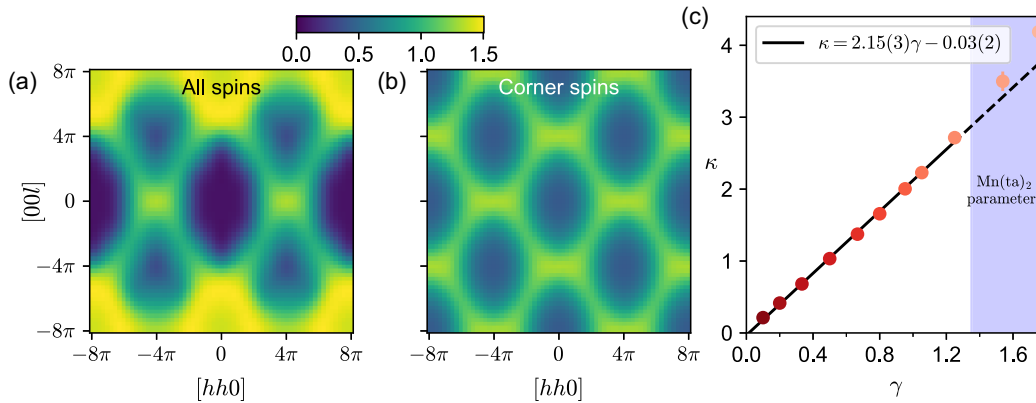


FIG. 3. Spin structure factor from large-scale MC simulations at $T = 1.5$ K, $\gamma = 1.5$ in the $[hhl]$ plane including all spins [(a)] and only sites residing at the corners of tetrahedra [(b)]. Finite width bowties at $\mathbf{q} = (\pm 4\pi, \pm 4\pi, 0)$ are found in both and the structure factor in (b) is within 1% of that found at $T = 0.07$ K. (c) The width of the bowties in the structure factor of the effective field parametrized by κ [see Eq. (6)] for different values of the coupling ratio γ at $T = 0.07$ K. A linear fit was performed to the data up to $\gamma = 1.25$ (black line).

number of magnetically disordered degrees of freedom (in fact, higher than for most known spin liquids), a reasonably large Ramirez frustration ratio, and a structure factor reflecting Coulomb physics in the presence of charges controlled through γ . Experimentally, external pressure may be a viable tool for controlling γ , similar to spin-1/2 frustrated magnets [38,39]. The consequences of this picture for the inelastic spectrum and the nature of excitations are interesting open questions. Inspired by routes taken for the pyrochlores [12,28,40], ways to build a multitude of exotic phases by taking a selection of degrees of freedom out of the ground state, e.g., via chemical substitution or with magnetic field, can be thought of. Even more broadly, $[\text{Mn}(\text{ta})_2]$ belongs to a family of metal-azolate frameworks, whose potential for low-energy physics remained until recently to a large extent uncharted. These frameworks provide a versatile platform to engineer (quantum) frustrated magnetism on the centered pyrochlore lattice and beyond, such as $[\text{Fe}(\text{ta})_2(\text{BF}_4)_x]$ with a degree of frustration $f \approx 27$ [19], $[\text{Cu}(\text{ta})_2]$ with Cu(II) dimers at low temperature [18], and $[\text{Cr}(\text{II/III})(\text{ta})_2(\text{CF}_3\text{SO}_3)_{0.33}]$ with large exchange couplings [21]. While ligand substitution in similar 1,2,3-triazolate-based Mn(II) networks is known to

influence their magnetic properties [41], guest molecule loading in the framework pores should further potentiate the adjustment possibilities in such materials. Thus, they offer us a near infinite playground for design and experimental characterization.

Acknowledgments. We are grateful to Nic Shannon for stimulating discussions. D.V. and R.R.-O. are grateful for financial support from DFG Grant No. VO-829/12-2 (DFG Priority Program 1928 “Coordination Networks: Building Blocks for Functional Systems”) and SEM micrographs taken by Ralph Freund. A.A.T., A.J., P.G., and H.-A. K.v.N. were supported by the German Research Foundation via TRR80. L.D.C.J. acknowledges financial support from the “Agence Nationale de la Recherche” under Grant No. ANR-18-CE30-0011-01. R.P.N., L.P., and L.D.C.J. acknowledge financial support from the LMU-Bordeaux Research Cooperation Program. R.P.N. and L.P. acknowledge support from FP7/ERC Consolidator Grant QSIMCORR, No. 771891, and the Deutsche Forschungsgemeinschaft (DFG, German Research Foundation) under Germany’s Excellence Strategy – EXC-2111 – 390814868. Our simulations make use of the ALPSCore library [42].

- [1] C. Castelnovo, R. Moessner, and S. Sondhi, Spin ice, fractionalization, and topological order, *Annu. Rev. Condens. Matter Phys.* **3**, 35 (2012).
- [2] *Spin Ice*, edited by L. D. C. Jaubert and M. Udagawa, Springer Series in Solid-State Sciences Vol. 197 (Springer, Berlin, 2021).
- [3] L. Savary and L. Balents, Quantum spin liquids, *Rep. Prog. Phys.* **80**, 016502 (2017).
- [4] Y. Zhou, K. Kanoda, and T.-K. Ng, Quantum spin liquid states, *Rev. Mod. Phys.* **89**, 025003 (2017).
- [5] J. Knolle and R. Moessner, A field guide to spin liquids, *Annu. Rev. Condens. Matter Phys.* **10**, 451 (2019).
- [6] S. V. Isakov, K. Gregor, R. Moessner, and S. L. Sondhi, Dipolar Spin Correlations in Classical Pyrochlore Magnets, *Phys. Rev. Lett.* **93**, 167204 (2004).
- [7] C. L. Henley, The “Coulomb phase” in frustrated systems, *Annu. Rev. Condens. Matter Phys.* **1**, 179 (2010).
- [8] S. T. Bramwell and M. J. Harris, The history of spin ice, *J. Phys.: Condens. Matter* **32**, 374010 (2020).
- [9] C. Castelnovo, R. Moessner, and S. L. Sondhi, Magnetic monopoles in spin ice, *Nature (London)* **451**, 42 (2008).
- [10] K. W. Plumb, H. J. Changlani, A. Scheie, S. Zhang, J. W. Krizan, J. A. Rodriguez-Rivera, Y. Qiu, B. Winn, R. J. Cava, and C. L. Broholm, Continuum of quantum fluctuations in a three-dimensional $S = 1$ Heisenberg magnet, *Nat. Phys.* **15**, 54 (2019).
- [11] A. M. Hallas, J. Gaudet, and B. D. Gaulin, Experimental insights into ground-state selection of quantum XY pyrochlores, *Annu. Rev. Condens. Matter Phys.* **9**, 105 (2018).

- [12] J. G. Rau and M. J. Gingras, Frustrated quantum rare-earth pyrochlores, *Annu. Rev. Condens. Matter Phys.* **10**, 357 (2019).
- [13] S. Trebst and C. Hickey, Kitaev materials, *Phys. Rep.* **950**, 1 (2022).
- [14] E. Kermarrec, R. Kumar, G. Bernard, R. Hénaff, P. Mendels, F. Bert, P. L. Paulose, B. K. Hazra, and B. Koteswararao, Classical Spin Liquid State in the $S = \frac{5}{2}$ Heisenberg Kagome Antiferromagnet $\text{Li}_9\text{Fe}_3(\text{P}_2\text{O}_7)_3(\text{PO}_4)_2$, *Phys. Rev. Lett.* **127**, 157202 (2021).
- [15] J. M. Bulled, J. A. M. Paddison, A. Wildes, E. Lhotel, S. J. Cassidy, B. Pato-Doldán, L. C. Gómez-Aguirre, P. J. Saines, and A. L. Goodwin, Geometric Frustration on the Trillium Lattice in a Magnetic Metal-Organic Framework, *Phys. Rev. Lett.* **128**, 177201 (2022).
- [16] X.-H. Zhou, Y.-H. Peng, X.-D. Du, J.-L. Zuo, and X.-Z. You, Hydrothermal syntheses and structures of three novel coordination polymers assembled from 1,2,3-triazolate ligands, *CrystEngComm* **11**, 1964 (2009).
- [17] F. Gándara, F. J. Uribe-Romo, D. K. Britt, H. Furukawa, L. Lei, R. Cheng, X. Duan, M. O’Keeffe, and O. M. Yaghi, Porous, conductive metal-triazolates and their structural elucidation by the charge-flipping method, *Chem. Eur. J.* **18**, 10595 (2012).
- [18] M. Grzywa, D. Denysenko, J. Hanss, E.-W. Scheidt, W. Scherer, M. Weil, and D. Volkmer, CuN_6 Jahn–Teller centers in coordination frameworks comprising fully condensed Kuratowski-type secondary building units: Phase transitions and magneto-structural correlations, *Dalton Trans.* **41**, 4239 (2012).
- [19] J. G. Park, M. L. Aubrey, J. Oktawiec, K. Chakarawet, L. E. Darago, F. Grandjean, G. J. Long, and J. R. Long, Charge delocalization and bulk electronic conductivity in the mixed-valence metal–organic framework $\text{Fe}(1,2,3\text{-triazolate})_2(\text{BF}_4)_x$, *J. Am. Chem. Soc.* **140**, 8526 (2018).
- [20] M. Grzywa, R. Röß-Ohlenroth, C. Muschielok, H. Oberhofer, A. Błachowski, J. Żukrowski, D. Vieweg, H.-A. K. von Nidda, and D. Volkmer, Cooperative large-hysteresis spin-crossover transition in the iron(II) triazolate $[\text{Fe}(\text{ta})_2]$ metal–organic framework, *Inorg. Chem.* **59**, 10501 (2020).
- [21] J. G. Park, B. A. Collins, L. E. Darago, T. Runčevski, M. E. Ziebel, M. L. Aubrey, H. Z. H. Jiang, E. Velasquez, M. A. Green, J. D. Goodpaster, and J. R. Long, Magnetic ordering through itinerant ferromagnetism in a metal–organic framework, *Nat. Chem.* **13**, 594 (2021).
- [22] R. A. Borzi, D. Slobinsky, and S. A. Grigera, Charge Ordering in a Pure Spin Model: Dipolar Spin Ice, *Phys. Rev. Lett.* **111**, 147204 (2013).
- [23] D. Slobinsky, G. Baglietto, and R. A. Borzi, Charge and spin correlations in the monopole liquid, *Phys. Rev. B* **97**, 174422 (2018).
- [24] C.-T. He, Z.-M. Ye, Y.-T. Xu, D.-D. Zhou, H.-L. Zhou, D. Chen, J.-P. Zhang, and X.-M. Chen, Hyperfine adjustment of flexible pore-surface pockets enables smart recognition of gas size and quadrupole moment, *Chem. Sci.* **8**, 7560 (2017).
- [25] L. Sun, C. H. Hendon, S. S. Park, Y. Tulchinsky, R. Wan, F. Wang, A. Walsh, and M. Dincă, Is iron unique in promoting electrical conductivity in MOFs?, *Chem. Sci.* **8**, 4450 (2017).
- [26] See Supplemental Material at <http://link.aps.org/supplemental/10.1103/PhysRevResearch.5.L022018> for details of synthesis, crystallographic characterization, thermodynamic measurements, DFT calculations, MC simulations, and the effect of dipolar interactions.
- [27] B. Javanparast, Z. Hao, M. Enjalran, and M. J. P. Gingras, Fluctuation-Driven Selection at Criticality in a Frustrated Magnetic System: The Case of Multiple- \mathbf{k} Partial Order on the Pyrochlore Lattice, *Phys. Rev. Lett.* **114**, 130601 (2015).
- [28] H. Yan, O. Benton, L. D. C. Jaubert, and N. Shannon, Theory of multiple-phase competition in pyrochlore magnets with anisotropic exchange with application to $\text{Yb}_2\text{Ti}_2\text{O}_7$, $\text{Er}_2\text{Ti}_2\text{O}_7$, and $\text{Er}_2\text{Sn}_2\text{O}_7$, *Phys. Rev. B* **95**, 094422 (2017).
- [29] S. Zhang, H. J. Changlani, K. W. Plumb, O. Tchernyshyov, and R. Moessner, Dynamical Structure Factor of the Three-Dimensional Quantum Spin Liquid Candidate $\text{NaCaNi}_2\text{F}_7$, *Phys. Rev. Lett.* **122**, 167203 (2019).
- [30] A. M. Samarakoon, K. Barros, Y. W. Li, M. Eisenbach, Q. Zhang, F. Ye, V. Sharma, Z. L. Dun, H. Zhou, S. A. Grigera, C. D. Batista, and D. A. Tennant, Machine-learning-assisted insight into spin ice $\text{Dy}_2\text{Ti}_2\text{O}_7$, *Nat. Commun.* **11**, 892 (2020).
- [31] D. R. Yahne, D. Pereira, L. D. C. Jaubert, L. D. Sanjeeva, M. Powell, J. W. Kolis, G. Xu, M. Enjalran, M. J. P. Gingras, and K. A. Ross, Understanding Reentrance in Frustrated Magnets: The Case of the $\text{Er}_2\text{Sn}_2\text{O}_7$ Pyrochlore, *Phys. Rev. Lett.* **127**, 277206 (2021).
- [32] S. M. Winter, A. A. Tsirlin, M. Daghofer, J. van den Brink, Y. Singh, P. Gegenwart, and R. Valentí, Models and materials for generalized Kitaev magnetism, *J. Phys.: Condens. Matter* **29**, 493002 (2017).
- [33] R. Moessner and J. T. Chalker, Low-temperature properties of classical geometrically frustrated antiferromagnets, *Phys. Rev. B* **58**, 12049 (1998).
- [34] J. N. Reimers, A. J. Berlinsky, and A.-C. Shi, Mean-field approach to magnetic ordering in highly frustrated pyrochlores, *Phys. Rev. B* **43**, 865 (1991).
- [35] R. P. Nutakki, L. D. C. Jaubert, and L. Pollet, The classical heisenberg model on the centred pyrochlore lattice, *arXiv:2303.11010*.
- [36] Y. Levin, Electrostatic correlations: From plasma to biology, *Rep. Prog. Phys.* **65**, 1577 (2002).
- [37] C. Castelnovo, R. Moessner, and S. L. Sondhi, Debye-Hückel theory for spin ice at low temperature, *Phys. Rev. B* **84**, 144435 (2011).
- [38] E. Kermarrec, J. Gaudet, K. Fritsch, R. Khasanov, Z. Guguchia, C. Ritter, K. A. Ross, H. A. Dabkowska, and B. D. Gaulin, Ground state selection under pressure in the quantum pyrochlore magnet $\text{Yb}_2\text{Ti}_2\text{O}_7$, *Nat. Commun.* **8**, 14810 (2017).
- [39] M. E. Zayed, C. Rüegg, J. Larrea J., A. M. Läuchli, C. Panagopoulos, S. S. Saxena, M. Ellerby, D. F. McMorrow, T. Strässle, S. Klotz, G. Hamel, R. A. Sadykov, V. Pomjakushin, M. Boehm, M. Jiménez-Ruiz, A. Schneidewind, E. Pomjakushina, M. Stingaciu, K. Conder, and H. M. Rønnow, 4-spin plaquette singlet state in the Shastry–Sutherland compound $\text{SrCu}_2(\text{BO}_3)_2$, *Nat. Phys.* **13**, 962 (2017).
- [40] K. A. Ross, L. Savary, B. D. Gaulin, and L. Balents, Quantum Excitations in Quantum Spin Ice, *Phys. Rev. X* **1**, 021002 (2011).
- [41] R. Röß-Ohlenroth, M. Hirle, M. Kraft, A. Kalytta-Mewes, A. Jesche, H.-A. Krug von Nidda, and D. Volkmer, Synthesis, thermal stability and magnetic properties of an interpenetrated Mn(II) triazolate coordination framework, *Z. Anorg. Allg. Chem.* **648**, e202200153 (2022).

- [42] A. Gaenko, A. Antipov, G. Carcassi, T. Chen, X. Chen, Q. Dong, L. Gamper, J. Gukelberger, R. Igarashi, S. Iskakov, M. Könz, J. LeBlanc, R. Levy, P. Ma, J. Paki, H. Shinaoka, S. Todo, M. Troyer, and E. Gull, Updated core libraries of the ALPS project, [Comput. Phys. Commun.](#) **213**, 235 (2017).